
Networks are Slacking Off: Understanding Generalization Problem in Image Deraining

Jinjin Gu^{1,2} **Xianzheng Ma**¹ **Xiangtao Kong**^{1,3} **Yu Qiao**^{1,3} **Chao Dong**^{1,3,*}

¹ Shanghai AI Laboratory ² The University of Sydney

³ Shenzhen Institutes of Advanced Technology, Chinese Academy of Sciences

jinjin.gu@sydney.edu.au, xianzhengma@pjlab.org.cn

{xt.kong, yu.qiao, chao.dong}@siat.ac.cn

Abstract

Deep deraining networks, while successful in laboratory benchmarks, consistently encounter substantial generalization issues when deployed in real-world applications. A prevailing perspective in deep learning encourages the use of highly complex training data, with the expectation that a richer image content knowledge will facilitate overcoming the generalization problem. However, through comprehensive and systematic experimentation, we discovered that this strategy does not enhance the generalization capability of these networks. On the contrary, it exacerbates the tendency of networks to overfit to specific degradations. Our experiments reveal that better generalization in a deraining network can be achieved by simplifying the complexity of the training data. This is due to the networks are slacking off during training, that is, learning the least complex elements in the image content and degradation to minimize training loss. When the complexity of the background image is less than that of the rain streaks, the network will prioritize the reconstruction of the background, thereby avoiding overfitting to the rain patterns and resulting in improved generalization performance. Our research not only offers a valuable perspective and methodology for better understanding the generalization problem in low-level vision tasks, but also displays promising practical potential.

1 Introduction

The burgeoning progress in deep learning has ushered in a series of promising low-level vision networks that significantly surpass traditional methods in benchmark tests. However, the intrinsic overfitting issue has prevented these deep models from real-world applications, especially when the real degradation differs a lot from the training data. We call this dilemma the generalization problem. Image deraining, as a traditional and important low-level vision task that aims at removing the undesired rain streaks in an image, also faces a serious generalization performance problem. Existing deraining models tend to do nothing for the rain streaks that are beyond their training distribution. See Figure 1 for an example.

Despite its significance, the generalization problem in the context of deraining tasks is not comprehensively explored in existing literature. To propose effective solutions, it is imperative first to understand the underlying causes of these generalization performance issues. However, comprehending generalization in a low-level task is far from straightforward; it is not a simplistic extension of the generalization research conducted within high-level vision tasks. In this paper, our objective is to take the pioneering step towards a more profound understanding of this challenge.

*Corresponding author.

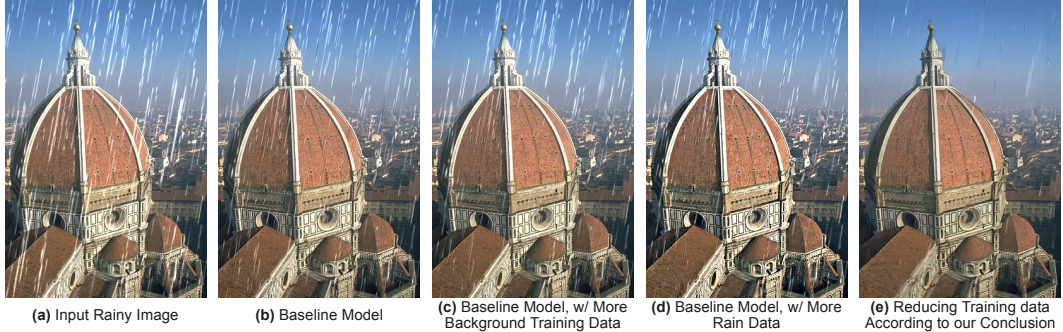


Figure 1: The existing deraining models suffer from severe generalization problems. After training with synthetic rainy images, when feeding (a) an image with different rain streaks, its output (b) shows a limited deraining effect. Two intuitive ways to improve generalization performance – (c) adding background images, and (d) adding rain patterns, cannot effectively relieve the generalization issue. In this paper, we provide a new counter-intuitive insight – (e) we improve the generalization ability of the deraining networks by selecting *much less* training background images for training.

As a quintessential decomposition problem, image deraining utilizes a relatively simple linear superimposition degradation model. When the network fails to generalize, rain streaks persist, while the image background may remain unaffected. This phenomenon, being intuitive and quantifiable, lends itself well to our research. Contrary to previous works that solely rely on overall image quality metrics, we propose a decoupling of the deraining task into two distinct components: rain removal and background reconstruction. These components are then separately analyzed. A key motivation behind this approach is the recognition that quality deterioration may result from either unsuccessful removal of rain streaks or poor reconstruction of the image background. Given that the generalization problem in the deraining task primarily pertains to the removal of rain streaks, our research methodology enables us to isolate and minimize the influence of extraneous factors.

In this paper, we argue that the generalization problem arises when the network overfits to the degradation, *i.e.*, the rain patterns present in the training set. One significant factor contributing to this outcome is the inappropriate training objective. We commence our analysis with the most fundamental element involved in formulating the training objective — the training data. Numerous studies have attempted to enhance real-world performance by increasing the complexity of training data. This approach originates from a natural but unproven “acknowledgement” in low-level vision that augmenting the quantity of training data can rectify the generalization problem. This “acknowledgement” has also permeated the deraining community, suggesting that a network exposed to a more diverse training set (both in terms of background images and rain streaks) will be better equipped to generalize to unseen scenarios. However, this approach does not effectively address the generalization problem in deraining. We contend that this issue arises precisely because the network is provided with an excess of background data during training. Consequently, the model fails to learn to reconstruct the image content and instead overfits to the degradation. By employing our analysis method, which separately measures background reconstruction and deraining effect, we arrive at some counter-intuitive conclusions.

Our key findings. We find that deep networks are slacking off during training, aiming to reduce the loss in the quickest way possible. This approach, unfortunately, leads to subpar generalization performance. The improper objective set for training serves as one of the primary contributors to this issue. Our finding can be summarized as:

In the task of separating image content from additive degradation, deep networks display a tendency to learn the less complex element.

Specifically, under common training settings where background complexity is high and rain complexity is low, the network naturally learns to identify and separate rain streaks, given that they are less complex and thus easier to learn. However, when real-world scenarios deviate from the trained depiction of rain, the network tends to disregard them, resulting in poor generalization performance. Conversely, when we train the model using a less complex background image set, it demonstrates superior generalization ability, as illustrated in Figure 1 (e). This may be attributed to the fact that when the complexity of the training image background is less than that of the rain patterns, the network will again take a shortcut to reduce the loss – in this case, by learning to reconstruct the background rather than overfitting to the rain streaks. It is important to note that the model’s

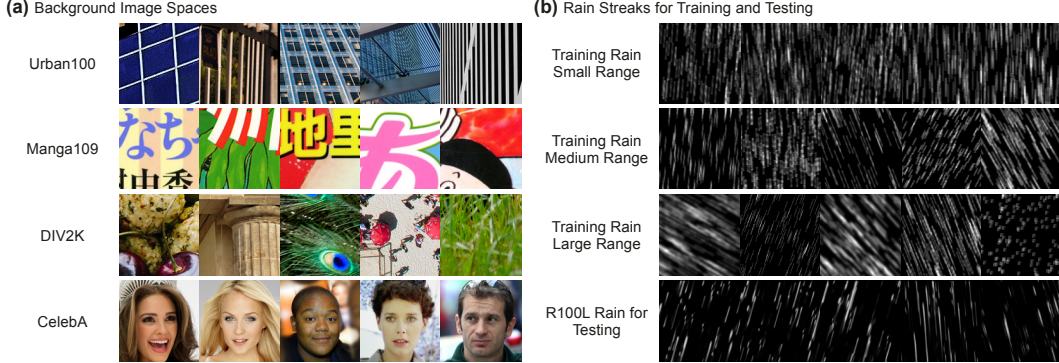


Figure 2: **(a)** Background images from different image datasets. It can be seen that the structure of the face image (CelebA) is relatively complex. Natural image patches (DIV2K) contain natural textures and patterns. The patterns in Manga109 and Urban100 are artificially created – Manga images have sharp edges, while Urban images contain a lot of repeating patterns and self-similarities. **(b)** Rain streaks used our experiments.

performance is determined not only by the removal of rain but also by the quality of background reconstruction. Reducing the background complexity of the training data might inevitably lead to subpar reconstruction outcomes. Nonetheless, our results reveal that a model trained on just 256 images can already handle most image components effectively. These counter-intuitive phenomena have not been previously studied or valued in the literature.

Implication. Our results offer intriguing and insightful contributions to the existing body of literature. They underscore the critical role of the training objective in determining a model’s generalization capabilities. An inappropriate and incomplete training objective creates a loophole for deep networks to “slack off”. While we anticipate that the network will learn the rich semantics inherent in natural images, it is often overlooked that the low-level vision system can also achieve learning objectives through shortcuts, which may, however, result in subpar generalization performance. Our findings also highlight that a model with robust generalization capabilities should learn the distribution of natural images, rather than overfitting to the degradation. Leveraging our insights, even the simplest networks can exhibit strong generalization capabilities, indicating the significant potential for practical application of our findings.

1.1 Related Works

This research primarily pertains to the field of deraining studies. However, unlike the majority of existing deraining research, we do not propose new network structures, loss functions, or datasets. Our objective is to analyze and understand the generalization problem within the context of the deraining task. Due to space constraints, reviews of deraining works are provided in the supplementary material. We will proceed to review previous works focusing on interpretability and understanding generalization in low-level vision.

Deep learning interpretability research aims to understand the mechanism of deep learning methods and to obtain clues about the success or failure of these methods. Without a deep understanding of these working mechanisms, we are not convinced to move forward in the right direction. The research on deep learning interpretability follows a long line of works, most focusing on the classification task [41; 42; 40; 43; 69; 32]. Low-level vision tasks have also embraced great success with powerful deep-learning techniques. There are also works on interpretability for these deep low-level networks [16; 55; 33; 38]. For the generalization problem in low-level vision, these problems often arise when the testing degradation does not match the training degradation, *e.g.*, different downsampling kernel [17; 27; 23] and noise distribution [19; 6]. The existing works either develop blind methods to include more degradation possibilities in the training process or make the training data closer to real-world applications. Only a little work has been proposed to study the reasons for this lack of generalization performance [29; 30]. More details of these previous works can also be found in supplementary material. No research has attempted to investigate the interpretation of the training process of low-level vision networks, especially from the perspective of the generalization problem.

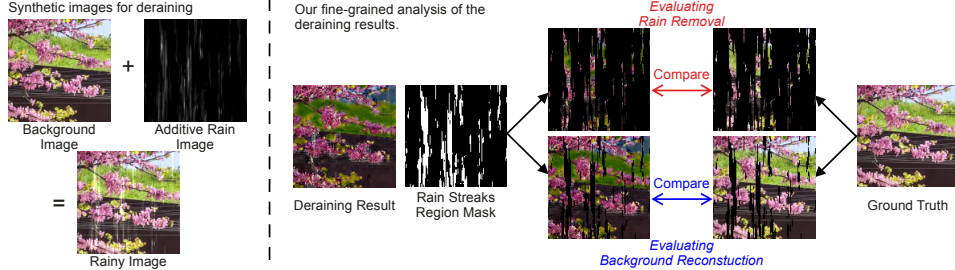


Figure 3: **(Left)** The illustration of the rainy image synthesis. **(Right)** Our fine-grained analysis of the deraining results.

2 Analysis Method

Our objective is to investigate how different training objectives influence network behavior and generalization performance. Prior to detailing our observations, this section will outline our experimental designs and quantitative analytical methods.

2.1 Construction of Training Objective

The training objective of a deep network is jointly determined by the training data and the loss function. We set a variety of training objectives in order to observe the changes in the generalization performance of different deraining models. As shown in Figure 3 (left), a rainy image O can be modelled using a linear model $O = B + R$, where B is the image background, and R is the additive rain streaks. We change the training objectives with different background images and rain streaks.

Background Images. Typically, image backgrounds are sampled from street view images [14] or natural image datasets [37; 1], as these images are close to the application scenarios of deraining. In literature, previous works [10; 65] claim that the model can learn the prior knowledge of reconstructing these scenes by training on a large number of such background images. We break this common sense by constructing different training background image sets from the following two aspects.

First, we change the number of training background images. The amount of training data partially determines the complexity of network learning. We argue that as too much background data are provided for training, the model cannot faithfully learn to reconstruct the image content but turn to overfit the degradation patterns. We reduce the complexity of the background images to see how the network behaviour changes in extreme scenarios. In our experiments, we use 8, 16, 32, 64, 128, 256, 512, and 1024 background image patches of size 128×128 to build the training datasets, respectively. We also use a large number of patches (up to 30,000) to simulate the common situation when the image background is sufficiently sampled.

In addition to the data scale, the image content will also affect network learning. For images with many self-similar or regular patterns, it is easier for the network to fit the distribution. While a face image that contains both short- and long-term dependent structures is apparently more complex than a skyscraper that consists of only repeated lines and grids [2]. We select image distribution as the second aspect of our dataset construction. We sample from four image datasets that are distinct from each other: CelebA (face images) [31], DIV2K (natural image patches) [44], Manga109 (comic image patches) [34], and Urban100 (building image patches) [21]. Some examples of these images are shown in Figure 2 (a).

Rain streaks synthesis. Since it is hard to collect a large number of real-world rainy/clean image pairs, we follow the previous deraining works [13; 10] to synthesize rainy images for research. We use two kinds of rain streaks for training and testing, separately. For training, we use the computational model² to render the streaks left on the image by raindrops of varying sizes, densities, falling speeds, and directions. This model allows us to sample rain streaks from different distributions. We adopt three rain image ranges for training, where different ranges may lead to different generalization effects, see Figure 2 (b) for a convenient visualization and Table 1 for the

Table 1: Different rain streaks settings.

Range	Quantity	Width	Length	Direction
Small	[200, 300]	{5}	[30, 31]	[−5°, 5°]
Medium	[200, 300]	{5, 7, 9}	[20, 40]	[−30°, 30°]
Large	[200, 300]	{1, 3, 5, 7, 9}	[5, 60]	[−70°, 70°]

²The re-implementation of the PhotoShop rain streaks synthesis method. Please refer to this link.

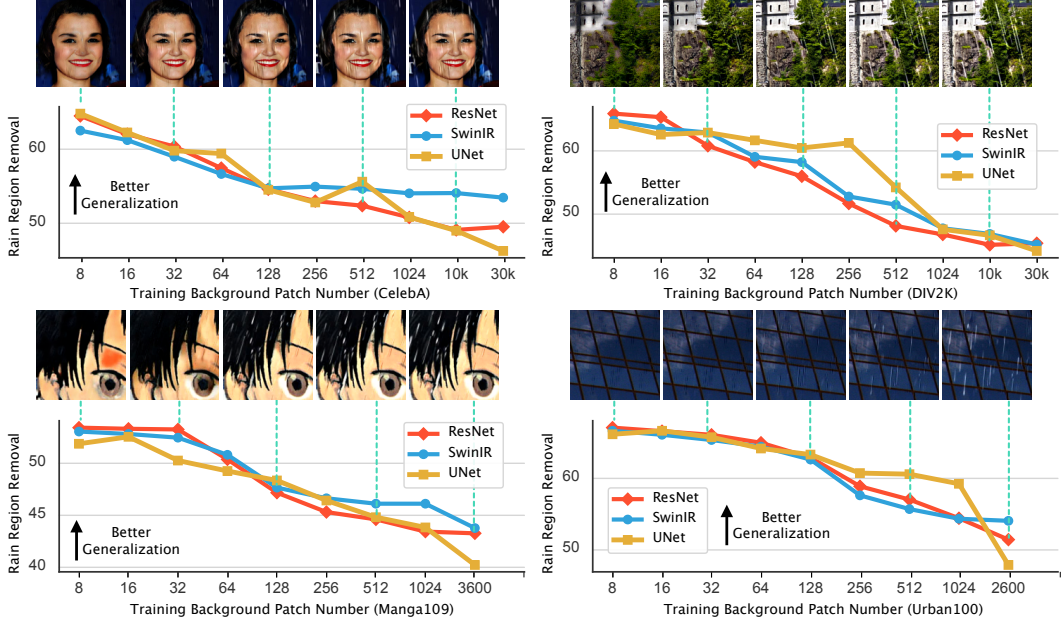


Figure 4: The relationship between the number of training patches and their rain removal performance. The x -axis represents the patch number, and the y -axis represents the rain removal effect E_R . Higher values on the y -axis mean better rain removal. The test rain patterns are not in the training set. The effect of rain removal at this time reflects the generalization performance. The qualitative results are obtained using ResNet.

detailed settings. For testing, we use the synthetic rain patterns in [57]. Although the rain streaks are visually similar to humans, they still pose a huge generalization challenge to existing models.

Loss Function. In low-level vision, the loss function is usually defined by the difference between the output image and the ground truth. In our study, we use the l_1 -norm loss, as it is the most commonly used and simplest loss function.

2.2 Decoupling Analysis of Rain Removal Results

Generally, the evaluation of a deraining model is to compute similarity metrics between the output and ground truth images [15]. However, such an evaluation of the whole image may lead to unfair comparison. For example, an image with perfect background reconstruction but inferior rain removal may have a higher PSNR value than that with perfect rain removal but a slightly flawed background reconstruction (e.g., color shift). Such quantitative results would introduce systematic errors.

In this work, we discuss the removal of rain streaks separately from the reconstruction of the background regions. The generalization performance of a deraining model is mainly shown in the form of removing unseen rain. The reconstruction of the background may affect the visual effect but is irrelevant to the removal of rain streaks. It can be seen that the pixels in R without rain streaks should be black, while rain streaks will appear brighter, as shown in Figure 2 (b). After synthesis, these black areas reflect the background area, while the brighter areas indicate the rainy regions. A perfect rain removal effect should do minimal damage to the background area and remove the additive signal from the rain streaks area. By processing the R to a binary mask M using a threshold t , where $M_{[i,j]} = 0$ if $R_{[i,j]} \leq t$ and $M_{[i,j]} = 1$ if $R_{[i,j]} > t$, we can segment the output image \tilde{O} into the rain streaks part $\tilde{O} \odot M$ and the background part $\tilde{O} \odot (1 - M)$. We then have two performance metrics:

- $E_R = \sqrt{\mathbb{E}[(\tilde{O} \odot M - O \odot M)^2]}$ gives the *Rain Removal Performance*. A network with poor generalization will not remove rain streaks. This term measures the changes made by the network in the rainy regions. A higher value reflects better rain removal performance.
- $E_B = \sqrt{\mathbb{E}[(\tilde{O} \odot (1 - M) - B \odot (1 - M))^2]}$ gives the effect of *Background Reconstruction* by comparing the background regions with the ground truth. A large error in this term means poor reconstruction quality.

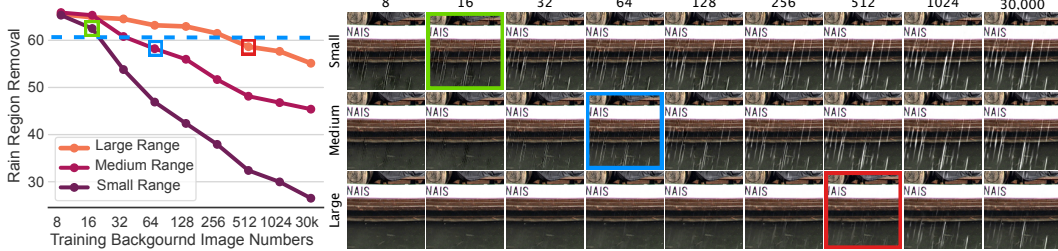


Figure 5: When trained with different rain ranges, the model exhibits different rain removal effects. The y -axis represents the quantitative rain removal effect. When the rain removal performance is lowered to the blue dashed line, the qualitative effect of removing rain starts to decrease significantly. We use ResNet in this experiment.

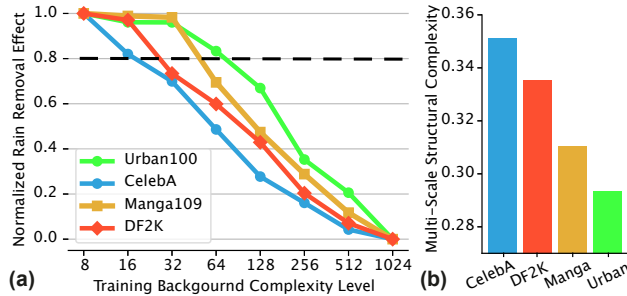


Figure 6: (a) The relationship between the number of training patches and their normalized rain removal performance. When the y value is lowered to the grey dashed line, the qualitative effect of removing rain starts to decrease significantly. (b) The averaged complexity of different image categories given by [2].

2.3 Deep Models

We summarize existing networks into three main categories. The first category is a network composed of convolutional layers and deep residual connections, and we use the ResNet [24] as a representative. The second category is the network with an encoder-decoder design, and we use UNet [36] as a representative. UNet introduces down-sampling and up-sampling layers to extract global and multi-scale features, which have been proven successful in many deraining networks. The last category is the image processing Transformer. Transformer [39; 67; 68] is a new network structure characterized by self-attention operations. We include SwinIR [26] as a representative Transformer in our study. For more training settings, please check the supplementary material.

3 Understanding Generalization

We next conduct experiments based on the above analysis methods. Our analysis consists of two aspects – the rain removal effect and the background reconstruction effect.

3.1 Generalization on Rain Removal

We conduct an analysis of the rain removal effect on unseen rain streaks. Importantly, since we use different types of rain streaks for training and testing, the results presented in this section all reflect generalization performance. After extensive experimentation, we arrive at the following observations.

Training with fewer background images leads to better deraining effect. Firstly, we maintain the range of rain streaks at the medium level, replacing the background images to construct different training objectives. Experiments are conducted across all four categories of images. For each category, we use a training set comprising different quantities of image patches. We then test the rain removal efficacy of these models. The test images utilize rain streaks proposed in [57]. The testing background images are sampled from the corresponding categories and are distinct from those in the training set. The experimental results are presented in Figure 4. Despite variations in background images and networks, these experimental results all speak to the same trend. Remarkably, the deraining models trained on merely eight image patches can effectively handle unseen rain streaks. Conversely, models trained with a large number of background patches fail to remove these rain streaks. *This observation deviates from conventional wisdom.* In between these two extreme states, the rain removal effect deteriorates with an increase in the number of training images. By the time the patch number reaches 256, the networks have already lost most of their rain-removal ability. As the number of patches increases from 1024 to 30,000, the rain removal effect does not change significantly – they all fail to remove unseen rain. This trend is also reflected in the qualitative results.

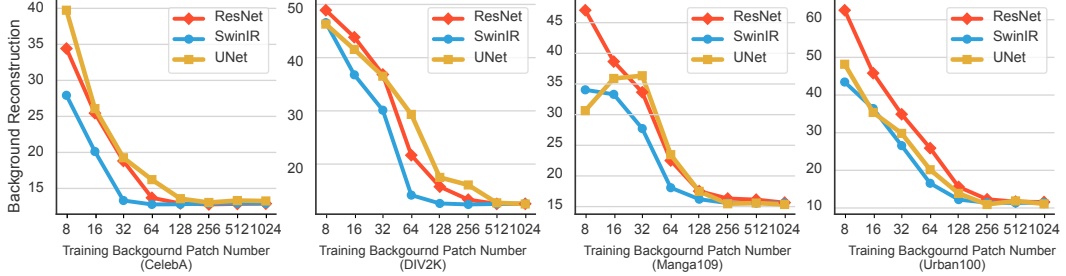


Figure 7: The relationship between the number of training patches and their background reconstruction effect. For each plot, the x -axis represents the patch number, and the y -axis represents the reconstruction error of the background.

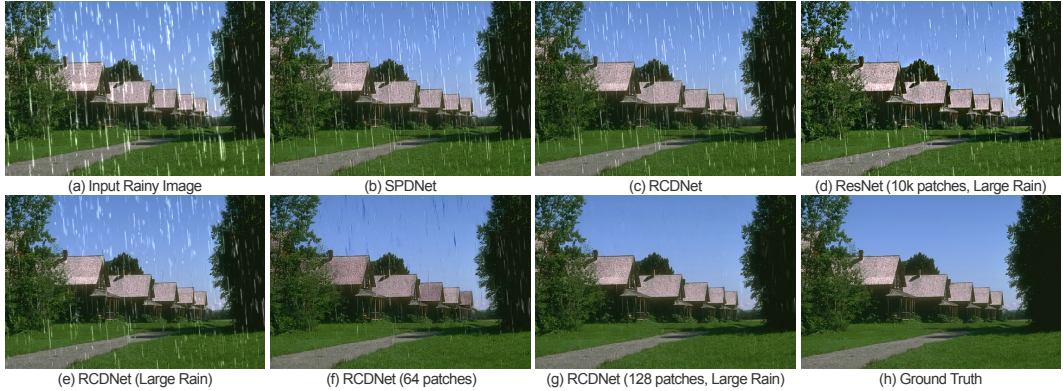


Figure 8: Visualization of the deraining results on a synthetic image. Zoom in for better comparison.

Here, we attempt to elucidate this intriguing phenomenon. Although we articulate the training objective as the removal of rain streaks from images (through the loss function), the network has two alternative strategies to minimize the training loss. The first strategy involves recognizing and removing rain streaks, while the second involves recognizing and reconstructing the image background. If the learning strategy is not specified, the network will “opt” for the simpler of these two strategies. When a large number of background patches are utilized in training, learning to reconstruct backgrounds becomes significantly more complex than learning to remove rain. Consequently, the network chooses to recognize and remove the rain. This decision, however, can lead to an overfitting problem: when new rain streaks differ from those used in training, the network fails to recognize and remove them. Conversely, when the background image comprises only a few image patches, learning the background becomes easier than learning rain streaks. In this scenario, the network recognizes image components in the background without overfitting to the features of rain streaks. As a result, the model demonstrates superior rain removal capabilities in images with unseen rain streaks.

The relative complexity between the background and rain determines the network behavior. To corroborate the aforementioned conjecture, we modify the range of the rain streaks used in training, as outlined in Section 2.1. When employing a medium rain range, the rain removal effect diminishes when training with 64 background patches. According to our explanation, a larger range of rain streaks complicates the network’s task of learning the rain pattern. As a result, the rain removal effect does not deteriorate until a larger number of background patches are used for training. The experimental results are depicted in Figure 5. It can be observed that, across all three training rain ranges, the rain removal effect decreases as the number of background patches increases. When a sufficient number of background images are used for training (30,000 patches), even a large training rain range fails to produce a model capable of achieving adequate rain removal performance. This suggests that the large rain range does not encompass our testing scenarios. When training with a large rain range, the network displays a significant drop in rain removal performance only when more than 512 background patches are used for training. Conversely, a model trained on a small rain range cannot exhibit satisfactory rain removal even with only 16 background training image patches. These results indicate that network behaviors are influenced by the relative relationship between the background image and rain streaks. The complexity or learning difficulty of the medium range rain is approximately less than that of 64 training background patches, while the complexity of the large

Training Objective Back.	Range	ResNet			SPDNet [62]			RCDNet [48]		
		$E_R \uparrow$	$E_B \downarrow$	$PSNR \uparrow$	$E_R \uparrow$	$E_B \downarrow$	$PSNR \uparrow$	$E_R \uparrow$	$E_B \downarrow$	$PSNR \uparrow$
30k	Medium	31.24	10.79	25.15	33.63	5.49	30.51	26.55	5.41	28.54
64	Medium	53.33	25.02	20.87	—	—	—	45.47	14.78	25.32
512	Large	—	—	—	39.88	8.91	28.57	37.53	7.16	29.60
256	Large	45.64	16.51	24.30	38.87	8.03	29.40	40.40	8.52	29.08
128	Large	51.75	23.53	21.45	43.20	14.59	25.67	44.67	13.72	26.09

Table 2: Quantitative comparisons between different models. \uparrow means the higher the better while \downarrow means the lower the better.

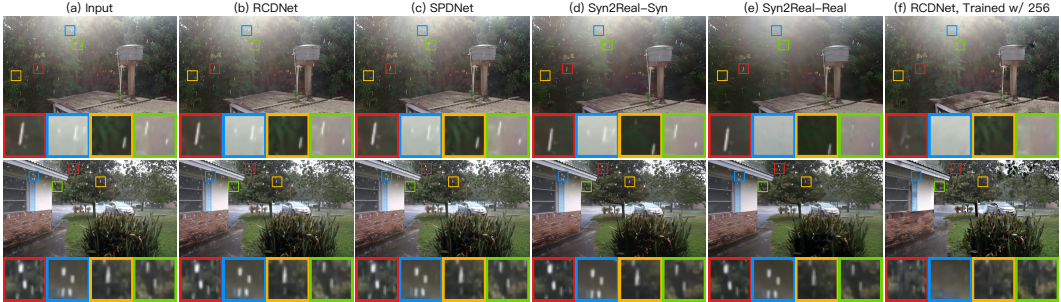


Figure 9: Qualitative results on real-world test images. Zoom in for better comparison.

range rain is approximately less than that of 512 training background patches. The network tends to take shortcuts, or “select” the easier learning pathway, depending on the situation.

A more complex background set makes it harder for the network to learn. We next modify the category of the background images used for training and monitor the resulting behaviors of the models. To facilitate comparison across different image categories, we normalize the deraining effect to a range between 0 and 1. The results are depicted in Figure 6 (a). The most intuitive conclusion is that, even when the number of training patches remains consistent, different image categories can lead to varying degrees of rain removal effectiveness. For instance, in the case of CelebA images, a jump from 8 to 16 patches results in a sharp decline in deraining performance. This contrast is evident when compared to natural image patches, where an increase to 16 patches does not result in a significant drop in rain removal performance. Moreover, for image patches sourced from Manga109 and Urban100, the rain removal performance does not exhibit a significant drop until the patch count exceeds 32. According to our interpretation, as the number of training patches increases, the more complex image categories will prompt the models to experience an earlier performance decline. Our results suggest that the complexity of these four image categories can be ranked, in ascending order, as CelebA, DIV2K, Manga109, and Urban100.

This ordering roughly aligns with our human perception. Face images, such as those in the CelebA set, exhibit strong global and local structures. DIV2K images, while rich in texture, possess a comparatively simple global structure. Manga images, on the other hand, lack complex textures but often contain text elements and intricate edges. Lastly, Urban images predominantly comprise repetitive patterns, such as stripes and grids. To corroborate our conclusion, we validate it using a complexity system derived from a mathematical model. Bagrov *et al.* [2] proposed a computational method for estimating the structural complexity of natural patterns, which includes natural images. We compute the multi-scale structural complexity for these four image categories, and the results corroborate our proposed ordering, as depicted in Figure 6 (b). This provides mathematical evidence to support our claim.

3.2 Reconstruction on Background

The aforementioned results indicate that the deraining capability can be enhanced by limiting the complexity of the background images used for training. However, utilizing only a restricted set of background images is not without its drawbacks. While it prevents the network from overfitting to rain patterns, it may conversely prompt the network to overfit to the limited selection of background images. We also conduct investigations to address this particular concern.

Using the decoupled evaluation metric E_B outlined in Section 2.2, we are able to independently assess the reconstruction of the background. The results, as depicted in Figure 7, show that as the number of training images increases, the quality of background reconstruction also improves. Remarkably, training with just 256 background patches can already yield a satisfactory background reconstruction effect. Adding more training images beyond this point does not lead to further performance improvements. These findings are surprising and counter-intuitive. We typically assume

that training low-level vision models requires a large number of images. However, our research suggests that training with an excessive number of background images does not necessarily enhance the reconstruction performance, but rather exacerbates the model’s tendency to overfit to rain streaks. Another unexpected result is that a model trained with merely 256 images can already handle most image components. This might imply that the complexity of image components and features for a low-level vision network might not be as high as traditionally believed.

4 Implication

This paper does not propose any new algorithms directly, but the conclusions drawn can provide insights on how to improve the removal of unknown rain streaks in existing models. Our experiments have yielded three significant practical findings: (1) By limiting the number of background images used in training, the network can focus more on learning the image content instead of overfitting to the rain streaks; (2) Enlarging the range of rain streaks in the training set can allow for the use of more background images in training; (3) Surprisingly, a small number of background images can already yield satisfactory reconstruction performance. These findings can be directly applied to enhance the generalization capabilities of existing models with minimal modifications. Our strategy is straightforward: *find a balance between the quantity of background images and the range of rain streaks in the training set to avoid overfitting to rain streaks.*

Some quantitative results are presented in Table 2. We use three deraining models as baselines (ResNet, SPDNet [62], RCDNet [48]) and demonstrate the power of the proposed simple strategy. We use 30,000 background images and the medium range rain to train our baseline models. The test set is the R100 dataset [57]. We quantify the deraining effect and the background reconstruction effect according to the decouple evaluation metrics E_R and E_B . We also test PSNR as a reference. It can be seen that using the existing training methods cannot generalize well to the unseen rain of R100, which is shown by the poor deraining performance in Table 2. However, due to the learning on a large number of images, the reconstruction errors of the baseline models are generally lower. Thus the PSNR values cannot objectively reflect the rain removal effect. We reduce the training background images to 64, which is the upper limit of the image number that can make the model generalize under medium range rain. At this time, the rain removal performance has greatly improved, but at the cost of background reconstruction performance. By enlarging the rain range and training with more background images, we are able to achieve a trade-off between rain removal performance and background reconstruction.

Figure 8 shows a qualitative comparison of these models under different training objectives. It can be seen that even with the advanced network structure design, the rain removal effects of the baseline models of SPDNet and RCDNet are not satisfactory. Using a larger range of rain can bring limited improvements. In the case of medium range rain, reducing the background image to 64 significantly improves the rain removal effect and results in unstable image reconstruction. When the rain range is enlarged, and the training background is set to 128 patches, the model can show excellent performance in rain removal and background reconstruction. Note that we do not use additional data or improve the network structure throughout the process. We only adjust the training data.

We also present the comparison on real images in Figure 9. In addition, semi-supervised methods [52; 20] have also been used to improve the deraining effect on real images, and we also include the representative method Syn2Real [60; 61]. Syn2Real-Syn is trained on synthetic data, and Syn2Real-Real is trained on synthetic labeled data and real unlabeled data. Due to the difference in the distribution of rain streaks, the models trained using synthetic data can not generate satisfactory rain removal effects. When obtaining some real images, Syn2Real-Real can indeed achieve some improvement. However, these improvements are not brought by improving the generalization ability. Because these methods manage to convert “rain outside the training set” to “rain inside the training set”. Since data collection is extremely difficult, this method still faces great challenges in practice. Our method improves generalization performance and achieves better results on test images.

5 Conclusion and Insights

We investigate the generalization problem in deraining networks. While our work focuses on image deraining, our key conclusions can provide insights for the wider field of low-level vision. We argue that the generalization problem in low-level vision cannot be attributed solely to insufficient network capacity. Rather, we discover that existing training strategies do not promote generalization. Networks tend to overfit the degradation patterns present in the training set, which leads to poor generalization

performance for unseen degradation patterns. Moreover, the current lack of effective interpretability tools for low-level vision models presents a significant obstacle. Without these tools, we struggle to understand what the low-level model is learning and why it learns in this way. This gap between the ideal and the reality compels us to reconsider the importance of interpretability in low-level vision networks. Our work provides a necessary perspective on this issue. These insights also need to be tested and validated in other low-level vision tasks. Our findings highlight the importance of continued research in this area, and we hope that our work will inspire further investigations.

References

- [1] Pablo Arbelaez, Michael Maire, Charless Fowlkes, and Jitendra Malik. Contour detection and hierarchical image segmentation. *IEEE transactions on pattern analysis and machine intelligence*, 33(5):898–916, 2010.
- [2] Andrey A Bagrov, Ilia A Iakovlev, Askar A Iliasov, Mikhail I Katsnelson, and Vladimir V Mazurenko. Multiscale structural complexity of natural patterns. *Proceedings of the National Academy of Sciences*, 117(48):30241–30251, 2020.
- [3] Yi Chang, Luxin Yan, and Sheng Zhong. Transformed low-rank model for line pattern noise removal. In *Proceedings of the IEEE international conference on computer vision*, page 1726–1734, 2017.
- [4] Chenghao Chen and Hao Li. Robust representation learning with feedback for single image deraining. In *Proceedings of the IEEE/CVF Conference on Computer Vision and Pattern Recognition*, page 7742–7751, 2021.
- [5] Hanting Chen, Yunhe Wang, Tianyu Guo, Chang Xu, Yiping Deng, Zhenhua Liu, Siwei Ma, Chunjing Xu, Chao Xu, and Wen Gao. Pre-trained image processing transformer. In *Proceedings of the IEEE/CVF Conference on Computer Vision and Pattern Recognition*, page 12299–12310, 2021.
- [6] Haoyu Chen, Jinjin Gu, Yihao Liu, Salma Abdel Magid, Chao Dong, Qiong Wang, Hanspeter Pfister, and Lei Zhu. Masked image training for generalizable deep image denoising. In *Proceedings of the IEEE/CVF Conference on Computer Vision and Pattern Recognition*, 2023.
- [7] Xiang Chen, Jinshan Pan, Kui Jiang, Yufeng Li, Yufeng Huang, Caihua Kong, Longgang Dai, and Zhentao Fan. Unpaired deep image deraining using dual contrastive learning. In *Proceedings of the IEEE/CVF Conference on Computer Vision and Pattern Recognition*, page 2017–2026, 2022.
- [8] Yingjun Du, Jun Xu, Xiantong Zhen, Ming-Ming Cheng, and Ling Shao. Conditional variational image deraining. *IEEE Transactions on Image Processing*, 29:6288–6301, 2020.
- [9] Xueyang Fu, Jiabin Huang, Xinghao Ding, Yinghao Liao, and John Paisley. Clearing the skies: A deep network architecture for single-image rain removal. *IEEE Transactions on Image Processing*, 26(6):2944–2956, 2017.
- [10] Xueyang Fu, Jiabin Huang, Delu Zeng, Yue Huang, Xinghao Ding, and John Paisley. Removing rain from single images via a deep detail network. In *Proceedings of the IEEE conference on computer vision and pattern recognition*, page 3855–3863, 2017.
- [11] Xueyang Fu, Borong Liang, Yue Huang, Xinghao Ding, and John Paisley. Lightweight pyramid networks for image deraining. *IEEE transactions on neural networks and learning systems*, 31(6):1794–1807, 2019.
- [12] Xueyang Fu, Qi Qi, Zheng-Jun Zha, Yurui Zhu, and Xinghao Ding. Rain streak removal via dual graph convolutional network. In *Proceedings of the AAAI Conference on Artificial Intelligence*, volume 35, page 1352–1360, 2021.
- [13] Kshitiz Garg and Shree K Nayar. Photorealistic rendering of rain streaks. *ACM Transactions on Graphics (TOG)*, 25(3):996–1002, 2006.
- [14] Andreas Geiger, Philip Lenz, and Raquel Urtasun. Are we ready for autonomous driving? the kitti vision benchmark suite. In *2012 IEEE conference on computer vision and pattern recognition*, pages 3354–3361. IEEE, 2012.
- [15] Jinjin Gu, Haoming Cai, Haoyu Chen, Xiaoxing Ye, Jimmy Ren, and Chao Dong. Pipal: a large-scale image quality assessment dataset for perceptual image restoration. In *European Conference on Computer Vision*, pages 633–651. Springer, 2020.

[16] Jinjin Gu and Chao Dong. Interpreting super-resolution networks with local attribution maps. In *Proceedings of the IEEE/CVF Conference on Computer Vision and Pattern Recognition*, pages 9199–9208, 2021.

[17] Jinjin Gu, Hannan Lu, Wangmeng Zuo, and Chao Dong. Blind super-resolution with iterative kernel correction. In *Proceedings of the IEEE/CVF Conference on Computer Vision and Pattern Recognition*, pages 1604–1613, 2019.

[18] Shuhang Gu, Deyu Meng, Wangmeng Zuo, and Lei Zhang. Joint convolutional analysis and synthesis sparse representation for single image layer separation. In *Proceedings of the IEEE International Conference on Computer Vision*, page 1708–1716, 2017.

[19] Shi Guo, Zifei Yan, Kai Zhang, Wangmeng Zuo, and Lei Zhang. Toward convolutional blind denoising of real photographs. In *Proceedings of the IEEE/CVF conference on computer vision and pattern recognition*, pages 1712–1722, 2019.

[20] Huaibo Huang, Aijing Yu, and Ran He. Memory oriented transfer learning for semi-supervised image deraining. In *Proceedings of the IEEE/CVF Conference on Computer Vision and Pattern Recognition*, pages 7732–7741, 2021.

[21] Jia-Bin Huang, Abhishek Singh, and Narendra Ahuja. Single image super-resolution from transformed self-exemplars. In *Proceedings of the IEEE conference on computer vision and pattern recognition*, pages 5197–5206, 2015.

[22] Kui Jiang, Zhongyuan Wang, Peng Yi, Chen Chen, Baojin Huang, Yimin Luo, Jiayi Ma, and Junjun Jiang. Multi-scale progressive fusion network for single image deraining. In *Proceedings of the IEEE/CVF conference on computer vision and pattern recognition*, page 8346–8355, 2020.

[23] Xiangtao Kong, Xina Liu, Jinjin Gu, Yu Qiao, and Chao Dong. Reflash dropout in image super-resolution. In *Proceedings of the IEEE/CVF Conference on Computer Vision and Pattern Recognition*, pages 6002–6012, 2022.

[24] Christian Ledig, Lucas Theis, Ferenc Huszár, Jose Caballero, Andrew Cunningham, Alejandro Acosta, Andrew Aitken, Alykhan Tejani, Johannes Totz, Zehan Wang, et al. Photo-realistic single image super-resolution using a generative adversarial network. In *Proceedings of the IEEE conference on computer vision and pattern recognition*, pages 4681–4690, 2017.

[25] Ruoteng Li, Loong-Fah Cheong, and Robby T Tan. Heavy rain image restoration: Integrating physics model and conditional adversarial learning. In *Proceedings of the IEEE/CVF Conference on Computer Vision and Pattern Recognition*, page 1633–1642, 2019.

[26] Jingyun Liang, Jiezhang Cao, Guolei Sun, Kai Zhang, Luc Van Gool, and Radu Timofte. Swinir: Image restoration using swin transformer. In *Proceedings of the IEEE/CVF International Conference on Computer Vision*, pages 1833–1844, 2021.

[27] Anran Liu, Yihao Liu, Jinjin Gu, Yu Qiao, and Chao Dong. Blind image super-resolution: A survey and beyond. *IEEE Transactions on Pattern Analysis and Machine Intelligence*, 2022.

[28] Xing Liu, Masanori Suganuma, Zhun Sun, and Takayuki Okatani. Dual residual networks leveraging the potential of paired operations for image restoration. In *Proceedings of the IEEE/CVF Conference on Computer Vision and Pattern Recognition*, page 7007–7016, 2019.

[29] Yihao Liu, Anran Liu, Jinjin Gu, Zhipeng Zhang, Wenhao Wu, Yu Qiao, and Chao Dong. Discovering "semantics" in super-resolution networks. *arXiv preprint arXiv:2108.00406*, 2021.

[30] Yihao Liu, Hengyuan Zhao, Jinjin Gu, Yu Qiao, and Chao Dong. Evaluating the generalization ability of super-resolution networks. *arXiv preprint arXiv:2205.07019*, 2022.

[31] Ziwei Liu, Ping Luo, Xiaogang Wang, and Xiaoou Tang. Deep learning face attributes in the wild. In *Proceedings of the IEEE international conference on computer vision*, pages 3730–3738, 2015.

[32] Scott M Lundberg and Su-In Lee. A unified approach to interpreting model predictions. *Advances in neural information processing systems*, 30, 2017.

[33] Salma Abdel Magid, Zudi Lin, Donglai Wei, Yulun Zhang, Jinjin Gu, and Hanspeter Pfister. Texture-based error analysis for image super-resolution. In *Proceedings of the IEEE/CVF Conference on Computer Vision and Pattern Recognition*, pages 2118–2127, 2022.

[34] Yusuke Matsui, Kota Ito, Yuji Aramaki, Azuma Fujimoto, Toru Ogawa, Toshihiko Yamasaki, and Kiyoharu Aizawa. Sketch-based manga retrieval using manga109 dataset. *Multimedia Tools and Applications*, 76(20):21811–21838, 2017.

[35] Dongwei Ren, Wangmeng Zuo, Qinghua Hu, Pengfei Zhu, and Deyu Meng. Progressive image deraining networks: A better and simpler baseline. In *Proceedings of the IEEE/CVF Conference on Computer Vision and Pattern Recognition*, page 3937–3946, 2019.

[36] Olaf Ronneberger, Philipp Fischer, and Thomas Brox. U-net: Convolutional networks for biomedical image segmentation. In *International Conference on Medical image computing and computer-assisted intervention*, pages 234–241. Springer, 2015.

[37] Gerald Schaefer and Michal Stich. Ucid: An uncompressed color image database. In *Storage and Retrieval Methods and Applications for Multimedia 2004*, volume 5307, pages 472–480. SPIE, 2003.

[38] Shuwei Shi, Jinjin Gu, Liangbin Xie, Xintao Wang, Yujiu Yang, and Chao Dong. Rethinking alignment in video super-resolution transformers. In *Advances in Neural Information Processing Systems*, 2022.

[39] Shuwei Shi, Jinjin Gu, Liangbin Xie, Xintao Wang, Yujiu Yang, and Chao Dong. Rethinking alignment in video super-resolution transformers. *Advances in Neural Information Processing Systems*, 2022.

[40] Avanti Shrikumar, Peyton Greenside, and Anshul Kundaje. Learning important features through propagating activation differences. In *International conference on machine learning*, pages 3145–3153. PMLR, 2017.

[41] Karen Simonyan, Andrea Vedaldi, and Andrew Zisserman. Deep inside convolutional networks: Visualising image classification models and saliency maps. *arXiv preprint arXiv:1312.6034*, 2013.

[42] Jost Tobias Springenberg, Alexey Dosovitskiy, Thomas Brox, and Martin Riedmiller. Striving for simplicity: The all convolutional net. *arXiv preprint arXiv:1412.6806*, 2014.

[43] Mukund Sundararajan, Ankur Taly, and Qiqi Yan. Axiomatic attribution for deep networks. In *International conference on machine learning*, pages 3319–3328. PMLR, 2017.

[44] Radu Timofte, Eirikur Agustsson, Luc Van Gool, Ming-Hsuan Yang, and Lei Zhang. Ntire 2017 challenge on single image super-resolution: Methods and results. In *Proceedings of the IEEE conference on computer vision and pattern recognition workshops*, pages 114–125, 2017.

[45] Cong Wang, Yutong Wu, Zhixun Su, and Junyang Chen. Joint self-attention and scale-aggregation for self-calibrated deraining network. In *Proceedings of the 28th ACM International Conference on Multimedia*, page 2517–2525, 2020.

[46] Cong Wang, Xiaoying Xing, Yutong Wu, Zhixun Su, and Junyang Chen. Dcsfn: Deep cross-scale fusion network for single image rain removal. In *Proceedings of the 28th ACM international conference on multimedia*, page 1643–1651, 2020.

[47] Guoqing Wang, Changming Sun, and Arcot Sowmya. Erl-net: Entangled representation learning for single image de-raining. In *Proceedings of the IEEE/CVF International Conference on Computer Vision*, page 5644–5652, 2019.

[48] Hong Wang, Qi Xie, Qian Zhao, and Deyu Meng. A model-driven deep neural network for single image rain removal. In *Proceedings of the IEEE/CVF Conference on Computer Vision and Pattern Recognition*, page 3103–3112, 2020.

[49] Tianyu Wang, Xin Yang, Ke Xu, Shaozhe Chen, Qiang Zhang, and Rynson WH Lau. Spatial attentive single-image deraining with a high quality real rain dataset. In *Proceedings of the IEEE/CVF Conference on Computer Vision and Pattern Recognition*, page 12270–12279, 2019.

[50] Yinglong Wang, Yibing Song, Chao Ma, and Bing Zeng. Rethinking image deraining via rain streaks and vapors. In *European Conference on Computer Vision*, page 367–382. Springer, 2020.

[51] Zheng Wang, Jianwu Li, and Ge Song. Dtdn: Dual-task de-raining network. In *Proceedings of the 27th ACM international conference on multimedia*, page 1833–1841, 2019.

[52] Wei Wei, Deyu Meng, Qian Zhao, Zongben Xu, and Ying Wu. Semi-supervised transfer learning for image rain removal. In *Proceedings of the IEEE/CVF conference on computer vision and pattern recognition*, pages 3877–3886, 2019.

[53] Yanyan Wei, Zhao Zhang, Haijun Zhang, Richang Hong, and Meng Wang. A coarse-to-fine multi-stream hybrid deraining network for single image deraining. In *2019 IEEE international conference on data mining (ICDM)*, page 628–637. IEEE, 2019.

[54] Jie Xiao, Man Zhou, Xueyang Fu, Aiping Liu, and Zheng-Jun Zha. Improving de-raining generalization via neural reorganization. In *Proceedings of the IEEE/CVF International Conference on Computer Vision*, page 4987–4996, 2021.

[55] Liangbin Xie, Xintao Wang, Chao Dong, Zhongang Qi, and Ying Shan. Finding discriminative filters for specific degradations in blind super-resolution. *Advances in Neural Information Processing Systems*, 34:51–61, 2021.

[56] Wenhan Yang, Jiaying Liu, Shuai Yang, and Zongming Guo. Scale-free single image deraining via visibility-enhanced recurrent wavelet learning. *IEEE Transactions on Image Processing*, 28(6):2948–2961, 2019.

[57] Wenhan Yang, Robby T Tan, Jiashi Feng, Jiaying Liu, Zongming Guo, and Shuicheng Yan. Deep joint rain detection and removal from a single image. In *Proceedings of the IEEE conference on computer vision and pattern recognition*, page 1357–1366, 2017.

[58] Youzhao Yang and Hong Lu. Single image deraining via recurrent hierarchy enhancement network. In *Proceedings of the 27th ACM International Conference on Multimedia*, page 1814–1822, 2019.

[59] Rajeev Yasarla and Vishal M Patel. Uncertainty guided multi-scale residual learning-using a cycle spinning cnn for single image de-raining. In *Proceedings of the IEEE/CVF conference on computer vision and pattern recognition*, page 8405–8414, 2019.

[60] Rajeev Yasarla, Vishwanath A Sindagi, and Vishal M Patel. Syn2real transfer learning for image deraining using gaussian processes. In *Proceedings of the IEEE/CVF conference on computer vision and pattern recognition*, page 2726–2736, 2020.

[61] Rajeev Yasarla, Vishwanath A Sindagi, and Vishal M Patel. Semi-supervised image deraining using gaussian processes. *IEEE Transactions on Image Processing*, 30:6570–6582, 2021.

[62] Qiaosi Yi, Juncheng Li, Qinyan Dai, Faming Fang, Guixu Zhang, and Tieyong Zeng. Structure-preserving deraining with residue channel prior guidance. In *Proceedings of the IEEE/CVF International Conference on Computer Vision*, pages 4238–4247, 2021.

[63] Weijiang Yu, Zhe Huang, Wayne Zhang, Litong Feng, and Nong Xiao. Gradual network for single image de-raining. In *Proceedings of the 27th ACM international conference on multimedia*, page 1795–1804, 2019.

[64] Syed Waqas Zamir, Aditya Arora, Salman Khan, Munawar Hayat, Fahad Shahbaz Khan, Ming-Hsuan Yang, and Ling Shao. Multi-stage progressive image restoration. In *Proceedings of the IEEE/CVF conference on computer vision and pattern recognition*, page 14821–14831, 2021.

[65] He Zhang and Vishal M Patel. Density-aware single image de-raining using a multi-stream dense network. In *Proceedings of the IEEE conference on computer vision and pattern recognition*, page 695–704, 2018.

[66] He Zhang, Vishwanath Sindagi, and Vishal M Patel. Image de-raining using a conditional generative adversarial network. *IEEE transactions on circuits and systems for video technology*, 30(11):3943–3956, 2019.

[67] Jiale Zhang, Yulun Zhang, Jinjin Gu, Yongbing Zhang, Linghe Kong, and Xin Yuan. Accurate image restoration with attention retractable transformer. In *International Conference on Learning Representations*, 2023.

[68] Chen Zheng, Yulun Zhang, Jinjin Gu, Yongbing Zhang, Linghe Kong, and Xin Yuan. Cross aggregation transformer for image restoration. In *Advances in Neural Information Processing Systems*, 2022.

[69] Bolei Zhou, David Bau, Aude Oliva, and Antonio Torralba. Interpreting deep visual representations via network dissection. *IEEE transactions on pattern analysis and machine intelligence*, 41(9):2131–2145, 2018.

[70] Man Zhou, Jie Xiao, Yifan Chang, Xueyang Fu, Aiping Liu, Jinshan Pan, and Zheng-Jun Zha. Image de-raining via continual learning. In *Proceedings of the IEEE/CVF Conference on Computer Vision and Pattern Recognition*, page 4907–4916, 2021.

[71] Lei Zhu, Chi-Wing Fu, Dani Lischinski, and Pheng-Ann Heng. Joint bi-layer optimization for single-image rain streak removal. In *Proceedings of the IEEE international conference on computer vision*, page 2526–2534, 2017.

Appendix

A Other Related Work

A.1 Image Deraining

Many methods have been proposed to develop state-of-the-art deraining networks. These works include deep networks designs [9; 47], residual networks [10; 28], recurrent networks [35; 58; 56], multi-task [51; 8] and multi-scale designs [22; 11; 59; 63; 53; 46; 64], sparsity-based image modeling [18; 71], low-rank prior [3], model-driven solutions [48; 50], attention mechanism [45; 5; 12], adversarial learning [25], representation learning [4], semi-supervised [60] and unsupervised learning [7]. Deep learning methods are data-hungry but collecting rain streaks and background image pairs are challenging. A lot of works have been proposed to synthesize rain streaks with better results. Garg *et al.* [13] first propose a physically-based photo-realistic rendering method for synthesizing rain streaks. Zhang *et al.* [65] and Fu *et al.* [9] use Photoshop software to manually add rain effects to images to build the synthetic paired data. Due to the poor generalization performance of existing methods, models trained on synthetic images were found to be ineffective in real-world scenarios. Some works [57; 66; 49] that have contributed to real collected deraining datasets. However, acquiring these datasets is still expensive and cannot solve the problem of poor generalization. There are also works that mentioned the generalization issue of the deraining models. Xiao *et al.* [54] and Zhou *et al.* [70] attempt to improve the generalization ability of deraining networks by accumulating knowledge from multiple synthetic rain datasets, as most existing methods can only learn the mapping on a single dataset for the deraining task. But this attempt does not allow the network to generalize beyond the training set.

In addition, semi-supervised methods [52; 20] have also been used to improve the deraining effect on real images, and we also include the representative method Syn2Real [60; 61]. There are some semi-supervised deraining methods [52; 20; 60; 61] are proposed to improve the performance of deraining models in real-world scenarios. When obtaining some real images similar to the test images, these works can indeed achieve some improvement. However, these improvements are not brought about by improving the generalization ability. Their solution is to include real test images in the training set, even if we don't have corresponding clean images. These methods are effective when we can determine the characteristics of the test image. But this does not solve the generalization problem. Because these methods manage to convert “rain outside the training set” to “rain inside the training set”. Since data collection is extremely difficult, this method still faces great challenges in practice.

A.2 Low-Level Vision Interpretability

We provide a detailed review of existing work on low-level visual interpretability. Gu and Dong [16] bring the first interpretability tool for super-resolution networks. Xie *et al.* [55] find the most discriminative filters for each specific degradation in a blind SR network, whose weights, positions, and connections are important for the specific function in blind SR. Magid *et al.* [33] use a texture classifier to assign patches with semantic labels, in order to identify global and local sources of SR errors. Shi *et al.* [39] show that Transformers can directly utilize multi-frame information from unaligned frames, and alignment methods are sometimes harmful to Transformers in video super-resolution. They use a lot of interpretability analysis methods in their work. The closest work to this paper is the deep degradation representation proposed by [29]. They argue that SR networks tend to overfit to degradations and show degradation “semantics” inside the network. The presence of these representations often means a decrease in generalization ability. The utilization of this knowledge can guide us to analyze and evaluate the generalization performance of SR methods [30].

B Transferability of Limited Training Patches

At the end of the main text, we propose a method to improve the generalization performance of the deraining network by reducing the number of training background image patches. However, this method will overfit the image content when the number of training background patches is very small. In the main text, we investigate the risk of reducing the number of training patches when testing on the same image category. Recall that with the increase of training images, the reconstruction of the background becomes better. Training with 256 background patches can already bring a good background reconstruction effect. Continuing to add training images does not further improve the performance of background reconstruction.

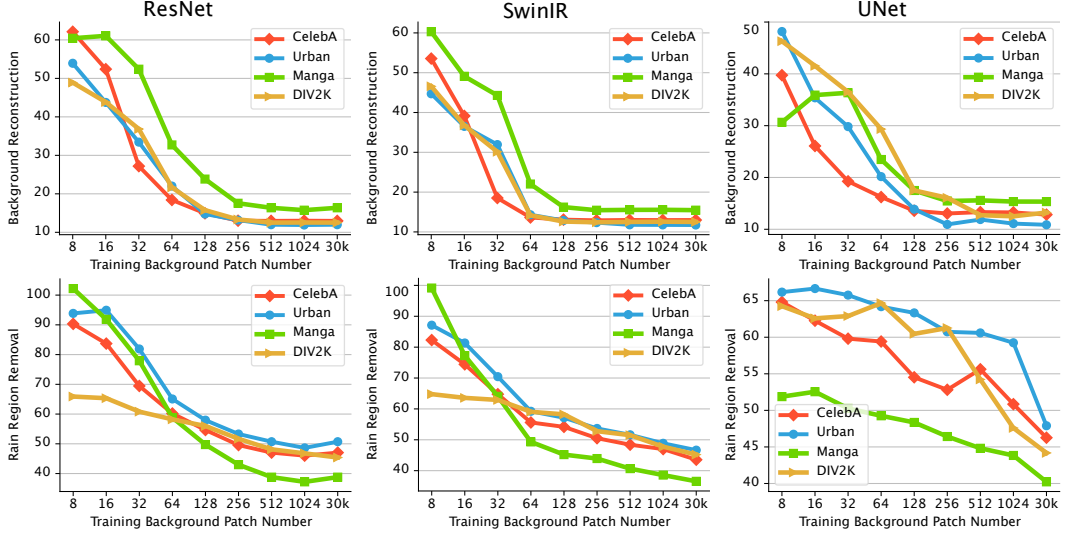


Figure 10: The relationship between the number of training patches and their rain removal or background reconstruction performance. The test image set for these six plots is the DIV2K set. We train the model with all four image categories to validate the performance when the image distribution mismatch. For background reconstruction E_B , lower values on the y -axis mean better background reconstruction. For rain removal effect E_R , higher values on the y -axis mean better rain removal. The test rain patterns are not in the training set. The effect of rain removal at this time reflects the generalization performance.

In this section, we investigate whether the proposed scheme is still robust when the training and testing patch distributions are significantly different. We train the model on four image categories and then test it using the DIV2K image category. This simulates the situation when the background image distribution differs from the test set. We observe the behavior of models trained with different numbers of patches. The results are shown in Figure 10. We can draw the following conclusions. First of all, even if the distribution of training background images is very different, the model trained using the images of CelebA and Urban categories can still perform similarly to the model trained by DIV2K patches. These models can reconstruct background images well when training patches reach 128 or more. At this time, the difference in the distribution of these training sets and DIV2K does not bring significant differences. The rain removal effect of these models is also similar. Second, we found that the model trained with Manga image patches differed from others. The model trained with manga image patches is generally worse at background reconstruction than other models. Even when the number of patches is large, the model trained on manga cannot achieve similar performance to other models. For rain removal, the model trained with manga also performs the worst. This result is in line with expectations because manga images are significantly different from other images, especially in the underlying image components. Although the other three types of images differ greatly in image structure, texture type and other characteristics, they all belong to the category of natural images. Whereas Manga images contain artificial textures and edges, which are quite different from other images.

There is a large image reconstruction error when training with images whose distribution is very different from that of the test set images. This is reasonable to some extent, because in this case, even using a large number of training images cannot bridge the error caused by this distribution mismatch. And we are pleased that the method of training using limited background images is robust to image content to a considerable extent, as long as the training images are natural images. This is consistent with our practice. In the process of actually using our method, we also found that as long as more than 256 image patches are used for training, the results are stable. There is no significant performance change due to the content of the selected training patches.

C More Results

We provide more results of different deraining models in Figure 11 and Figure 12. Note that we did not use additional data nor improve the network structure throughout the process. We only adjust

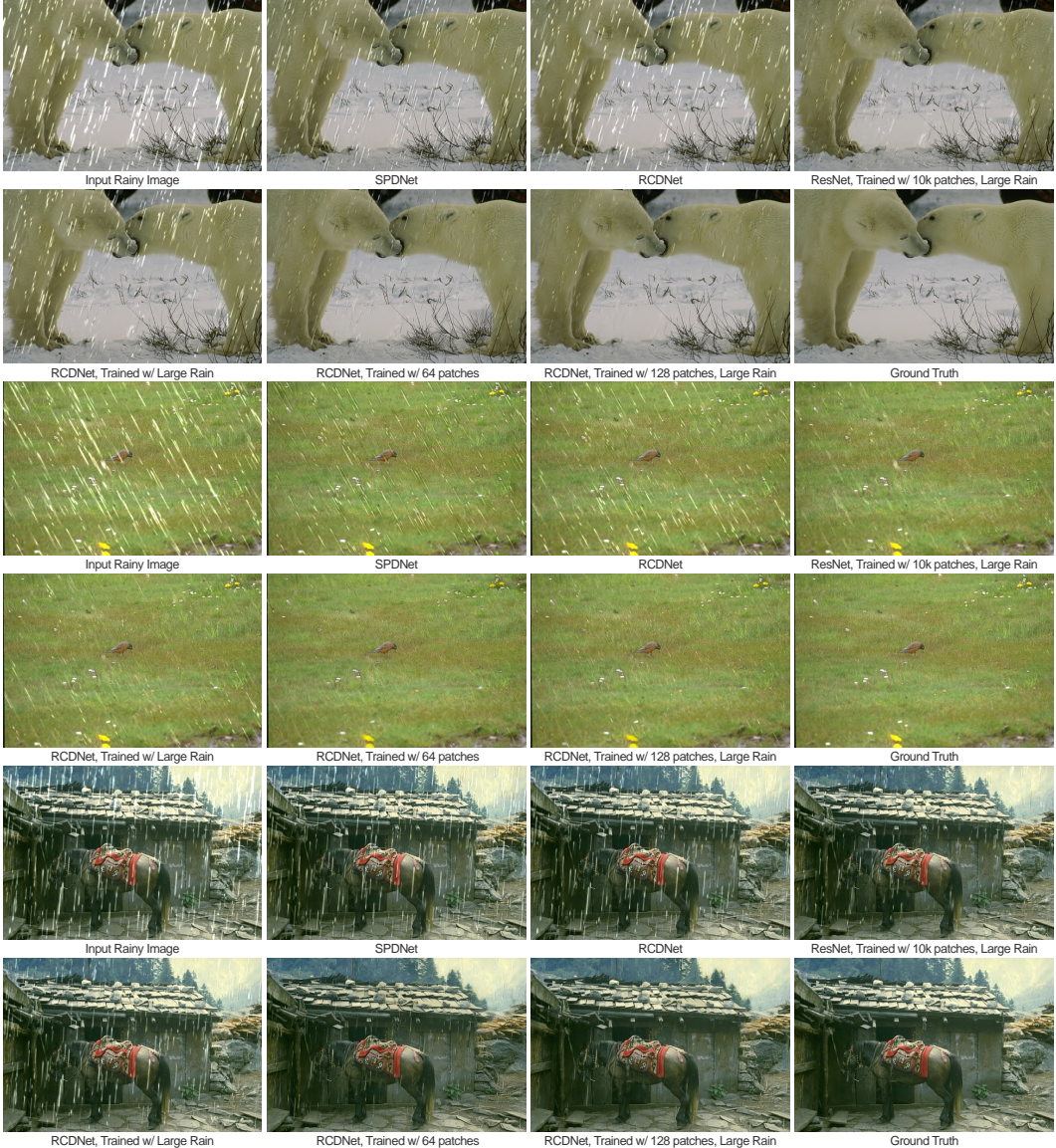


Figure 11: Visualization of the deraining results. Zoom in for better comparison.

the training objective. Although the effect of the output image can be further improved, it shows our conclusions’ practical value and application potential.

D Limitation.

Our work mainly takes the deraining task as a breakthrough point, and attempts to make a general summary of the generalization problem in low-level vision. Due to the differences between different low-level tasks, the analysis methods in this paper, especially the fine-grained analysis methods, may not be directly used on some other tasks. But we believe our work can still bring novel insights to the entire low-level vision field.

Our work also attempts to improve existing deraining models. But these improvements are based on the simple usage of some key conclusions of our work. Although shown effective, we believe that these methods are still far from ideal. We only demonstrate the application potential of the knowledge presented in this work and have no intention to propose state-of-the-art algorithms or models. Research efforts are still needed to develop more robust deraining algorithms using our conclusions.

E Reproducibility Statement

E.1 Resources

The models used in our work are taken directly from their respective official sources. Our code is built under the BasicSR framework <https://github.com/xinntao/BasicSR> for better code organization. The deraining model SPDNet is available at <https://github.com/Joyies/SPDNet>. The deraining model RCDNet is available at <https://github.com/hongwang01/RCDNet>. The training and testing datasets used in our work are all publicly available.

E.2 Network Training

Due to space constraints, we do not describe our training method in detail in the main text. Here we describe the training method to reproduce our results. A total of 150 models were involved in our experiments. We used the same training configuration for all models. We use Adam for training. The initial learning rate is 2×10^{-4} and $\beta_1 = 0.9$, $\beta_2 = 0.99$. For each network, we fixed the number of training iterations to 250,000. The batch size is 16, input rainy images are of size 128×128. The cosine annealing learning strategy is applied to adjust the learning rate. The period of cosine is 250,000 iterations. All models are built using the PyTorch framework and trained with NVIDIA A100 GPUs.

E.3 Availability

All the trained models and code will be publicly available.

F Ethics Statement

This study does not involve any human subjects, practices to data set releases, potentially harmful insights, methodologies and applications, potential conflicts of interest and sponsorship, discrimination/bias/fairness concerns, privacy and security issues, legal compliance, and research integrity issues. We do not anticipate any direct misuse of our contribution due to its theoretical nature.

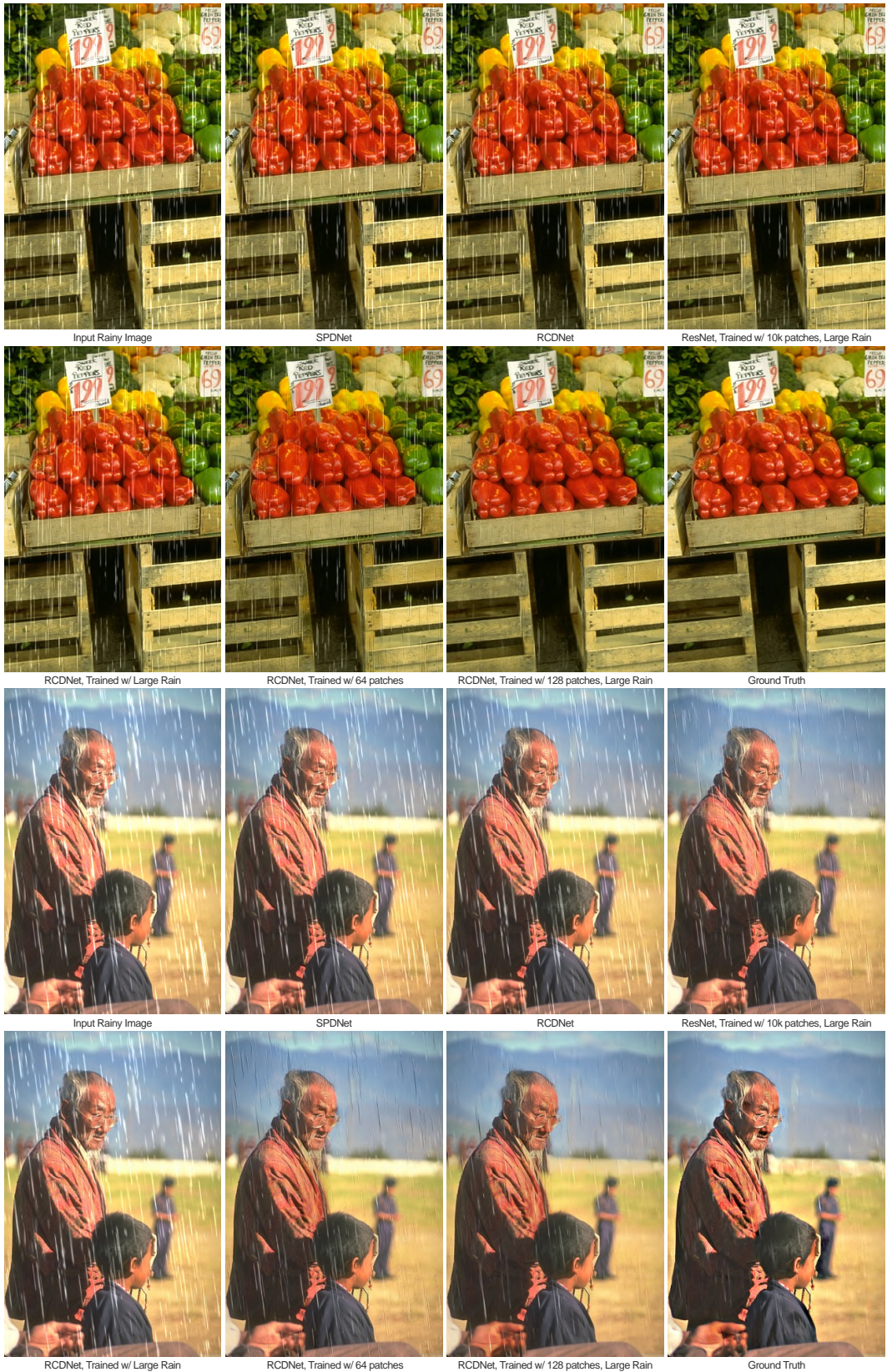


Figure 12: Visualization of the deraining results. Zoom in for better comparison.